Article

The n-10 fatty acids family in the lipidome of human prostatic adenocarcinoma cell membranes and extracellular vesicles

Carla Ferreri[1,*], Anna Sansone[1], Sandra Buratta[2], Lorena Urbanelli[2], Eva Costanzi[2], Carla Emiliani[2], and Chryssostomos Chatgilialoglu[1]

[1] Istituto per la Sintesi Organica e la Fotoreattività, Consiglio Nazionale delle Ricerche, ISOF, Area della Ricerca, Via P. Gobetti 101, 40129 Bologna (Italy); chrys@isof.cnr.it (C.C); anna.sansone@isof.cnr.it (A.S.)

[2] Department of Chemistry, Biology and Biotechnology, University of Perugia, Via del Giochetto, 06122 Perugia (Italy); sandra.buratta@unipg.it (S.B.); lorena.urbanelli@unipg.it (L.U.); eva.costanzi@studenti.unipg.it (E.C.); carla.emiliani@unipg.it (C.E.)

* Correspondence: carla.ferreri@isof.cnr.it (C.F.); Tel.: +39-051-6398289

Abstract: A new pathway leading to the n-10 fatty acid series has been recently evidenced, starting from sapienic acid - a monounsaturated fatty acid (MUFA) resulting from the transformation of palmitic acid by delta-6 desaturase. Sapienic acid attracts attention as novel marker of cancer cell plasticity. Here, we analyzed fatty acids including the n-10 fatty acid contents, and compared for the first time cell membranes and the corresponding extracellular vesicles (EV) of two human prostatic adenocarcinoma cell lines of different aggressiveness (PC3 and LNCaP). The n-10 components were 9-13% of the total fatty acids in both cancer cell lines and EVs, with total MUFA levels significantly higher in EVs of the most aggressive cell type (PC3). High sapienic/palmitoleic ratios indicated the preference for delta-6 *vs*. delta-9 desaturase enzymatic activity in these cell lines. The expressions analysis of enzymes involved in desaturation and elongation by qRT-PCR showed a higher desaturase activity in PC3 and a higher elongase activity toward polyunsaturated fatty acids than toward saturated fatty acids, compared to LNCaP cells. Our results improve the present knowledge in cancer fatty acid metabolism and lipid phenotypes, highlighting EV lipidomics to monitor positional fatty acid isomer profiles and MUFA levels in cancer.

Keywords: sebaleic acid, sapienic acid, positional fatty acid isomer, trans geometrical isomer, extracellular vesicle lipidome, desaturase enzyme, elongase enzyme, lipidomics

1. Introduction

Lipid biosynthesis and cancer cell growth are strongly connected each other in multiple aspects of replication, signaling and energy metabolism. Phospholipids are primary elements for cell membrane formation to ensure rapid duplication involved in carcinogenesis and invasiveness [1,2]. Follow-up of lipid metabolism in cancer cells clarified that not only a big quantity of lipids but also a specific quality of fatty acids is needed to provide structural and functional roles to cell membranes. It is well known that the biosynthesis of saturated fatty acids (SFA) and monounsaturated fatty acids (MUFA) starts from palmitic (C16:0) and stearic acids (C18:0), formed by the fatty acid synthase and elongase enzymes, followed by the delta-9 desaturase enzymatic step with the formation of palmitoleic (9cis-C16:1) and oleic (9cis-C18:1) acids, the latter being very good contributor of cell membrane fluidity [3,4]. Such membrane status triggers a cascade of proliferation signals maintaining stemness, tumour formation, and metastasis in breast, colon, and prostate cancers [5,6]. Recent attention has been given to the hexadecenoic MUFA family (C16:1) composed by the positional and geometrical isomers depicted in Figure 1. As shown in Figure 1, C16-derived MUFAs belong to three different fatty acid series, namely the n-7, n-9 and n-10 series, all formed from palmitic acid, which create structural, biochemical and biological diversities. They attracted interest both for their unambiguous identification methodology, to be used in biological samples, and for their intrinsic biological activities. The first and most studied is the n-7 component, palmitoleic acid,

evidenced by Cao and Hotamisligil for its lipokine-like activities [7]. Later on, its mitogen activity was reported [8] as well as its metabolism into an active compound in phagocytic cells [9]. This fatty acid is a known biomarker of desaturase activity in obesity [10] and risk of coronary heart disease found in the CAREMA cohort study [11]. In plasma lipoprotein fractions (triglycerides, cholesteryl esters and phospholipids) of healthy subjects we identified and quantified palmitoleic acid and, for the first time, its positional isomer of the n-10 series, sapienic acid (6cis-16:1), together with their corresponding trans geometrical isomers (9trans-C16:1 and 6trans-C16:1) [12]. We also described that morbidly obese subjects have statistically significant lower sapienic acid levels in plasma cholesteryl esters than healthy controls [13]. On the other hand, we observed that trans geometrical isomers of C16MUFAs can be used as valuable biomarkers of the endogenous free radical-based isomerization occurring during oxidative stress metabolism [14], since they are not relevantly present in foods.
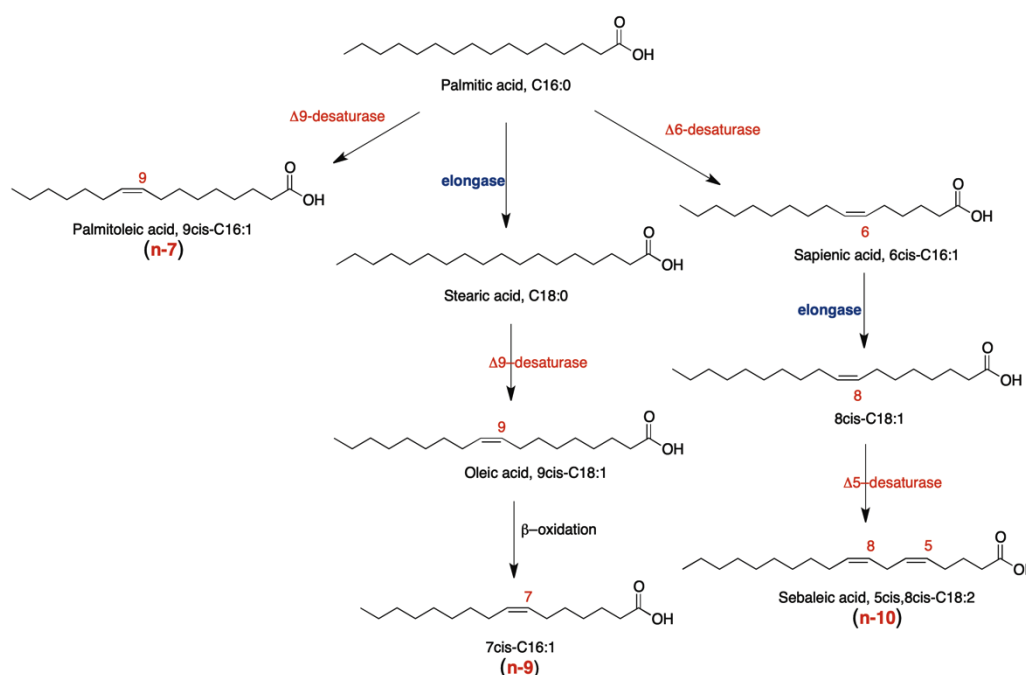

Figure 1- Main structures of the C16 MUFA family and their biosynthetic pathways starting from palmitic acid

Prouty and Pappas described sapienic acid as a typical fatty acid of human sebum, from where the name derives, highlighting the activity of delta-6 desaturase (FADS2) on palmitic acid [15]. This is an unusual metabolic pathway, since delta-6 desaturase works with omega-6 and omega-3 PUFAs as its natural substrates, and palmitic acid has a stronger affinity for delta-9 than for delta-6 desaturase. A high sapienic/palmitoleic acid ratio was observed only in primary sebocytes undergoing differentiation and lipogenesis (pediatric source), thus becoming similar to adult sebocytes [16]. Other known factors influencing the sapienic acid formation are the delta-9 desaturase inhibition [5] or its reduced transcription, as well as the decreased presence of linoleic acid, such as in case of an accelerated beta-oxidation in sebocytes, as thoroughly discussed by Prouty and Pappas [15]. After our detection of sapienic acid in human plasma, we were interested to study this fatty acid and its metabolism in human cancer cell lines. We reported for the first time in a human colon cancer cell line (Caco-2) that sapienic acid is present and leads to the formation of the n-10 fatty acid series. Indeed, after sapienic acid supplementation we characterized its metabolism, which occurs by a first elongase step to 8cis-C18:1 and a second delta-5 desaturase step to 5cis,8cis-C18:2 (sebaleic acid) (see Figure 1) [17]. Sebaleic acid is a positional isomer of the PUFA linoleic acid (9cis,12cis-C18:2) and deserves a careful consideration, since it is well known that the second double bond of natural fatty acids cannot be formed in eukaryotic cells so that PUFA cannot come from C18 MUFA. In fact, omega-6 and omega-3 C18 PUFA with two and three double bonds are essential fatty acids (EFA) for

humans, afforded exclusively by the diet and needed for life. Recently, sapienic acid was indicated as a marker of cancer plasticity, being individuated in high levels in other cancer cell lines, mouse hepatocellular carcinoma, and primary human liver and lung carcinomas [18], however no data were presented on its metabolism to PUFA. On the other hand, the importance of desaturase enzymes is very well assessed also as anticancer strategy [19] but the effects of a delta-6 desaturase activation on palmitic acid is not yet defined. We preliminary demonstrated by Laurdan two-photon microscopy that fluidity features change, comparing the two supplementations of the two positional isomers, palmitoleic and sapienic acids, to Caco-2 cells [17]. Since the n-10 fatty acids are present in membrane phospholipids, we thought that cell-derived extracellular vesicles (EVs) could be relevant indicators of their presence, adding this information to the other molecular insights under development as diagnostic and prognostic markers [20]. EV lipidomic profiles are reported by shotgun mass spectrometry but fatty acids of the same molecular mass and different position/geometry of one double bonds along the hydrocarbon chain are not distinguished [21,22]. Therefore, no information is available so far for the n-10 fatty acids in EVs.

Based on these premises, we decided to perform untargeted lipidomic analysis with specific attention to the n-10 fatty acid series in two human prostate cancer cell lines with a high and low metastatic potentials, PC3 and LNCaP respectively, widely studied for whole-genome sequencing [23], and their released EVs. Geometrical and positional isomers including n-10 fatty acids are new data of lipid metabolism in these cell lines and, in particular, in their EVs. In the present work we used analytical detection by GC (gas chromatography) and GC/MS (gas chromatography/mass spectrometry) under known conditions that allow separation and characterization of positional/geometrical isomers [17]. In parallel, elongation and desaturation enzyme expressions were determined in the two cell lines.

We anticipate that consistent differences were found in the two cell lines and their EVs regarding the n-10 fatty acid series, foreseeing further development for markers associated to cancer metabolism and metastatic potential. These findings expand the knowledge of fatty acid isomers in cancer lipid phenotypes that are important to be integrated in cancer–omic research.

2. Results

2.1. *Fatty acid profiles of PC3 and LNCaP cell lines*

Cultivation of PC3 and LNCaP cell lines was effected following literature procedures [24] and EVs were isolated from cell culture medium as described in Materials and methods. Cell membrane pellets of PC3 (n=8) and LNCaP (n=8) and corresponding PC3-EVs (n=8) and LNCaP-EVs (n=8) were first examined for the lipid classes, identifying phosphatidylethanolamine (PE), phosphatidylserine (PS), phosphatidylcholine (PC) together with cholesterol (CHO) and sphingomyelins (SM) by appropriate methods and standard references (Table S1 in Supplementary Information). Phospholipids (PE, PS, PC) have fatty acid residues and under known conditions of transesterification give fatty acid methyl esters (FAME) [12,13,17]. Fatty acids were recognized by appropriate standards and quantified by GC analysis as µg/mL (Table S2 of Supplementary Information; see Figures S1- S3 in Supplementary Information as representative examples of GC chromatograms and peak identification). From these quantitative data the percentages of each fatty acid in the total fatty acid content of PC3 and LNCaP cell membrane phospholipids and their EVs were obtained (% rel. quant.) and the values are shown in Tables 1 and 2 as mean ± s.e.m of n=8 replicates. First of all, we consider the fatty acid composition of cell membrane phospholipids shown in Table 1 with a particular interest for n-10 fatty acids, following sapienic acid to sebaleic acid transformation, in order to envisage differences of fatty acid composition between the two cell types. Interestingly, the n-10 fatty acids are present in both cell types reaching > 12% of the total fatty acids. Both cell types showed that the membrane content of sapienic acid is >3 times higher than palmitoleic acid, with palmitoleic acid being significantly lower in LNCaP than in PC3. As far as the

trans geometrical isomers are concerned, the trans isomer of sapienic acid was detected in a significantly higher quantity in LNCaP cells than in PC3. Regarding other fatty acids of the membrane profile, linoleic acid (C18:2 n-6) was found lower and arachidonic acids (C20:4 n-6) was found higher in LNCaP than in PC3.

Table 1. Fatty acid methyl esters (FAME) (%rel. quant.) obtained from membrane phospholipids of two different prostate cancer cell lines.

FAME[1]	PC3 (*n*=8)[2]	LNCaP (*n*=8)[2]
C14:0	3.26±0.32	3.44±0.17
C16:0	33.20±1.33	33.60±0.49
6*trans*-C16:1	0.36±0.04	0.56±0.03 **
6*cis*-C16:1 n-10	7.41±0.35	7.81±0.33
9 *cis*-C16:1 n-7	2.36±0.17	1.96±0.05 *
C18:0	10.92±0.54	11.48±0.25
9*trans*-C18:1	0.09±0.01	0.11±0.02
8*cis*-C18:1 n-10	5.98±0.75	4.55±0.12
9*cis*-C18:1 n-9	19.47±0.72	18.62±0.24
11*cis*-C18:1 n-7	3.92±0.30	3.90±0.08
5*cis*,8*cis*-C18:2 n-10	0.47±0.03	0.52±0.04
mono-*trans* C18:2 n-6	0.27±0.05	0.24±0.02
C18:2 n-6	2.48±0.19	1.97±0.08 *
C20:3 n-6	1.62±0.16	1.73±0.18
C20:4 n-6	2.86±0.23	4.01±0.14 ***
mono-*trans* C20:4	0.10±0.01	0.11±0.05
C20:5 n-3	0.47±0.06	0.37±0.07
C22:5 n-3	1.77±0.19	1.53±0.14
C22:6 n-3	2.98±0.18	3.49±0.20
SFA	47.38±1.39	48.52±0.46
MUFA	39.14±1.13	36.84±0.59
PUFA	12.65±0.37	13.62±0.42
n-6	6.96±0.34	7.70±0.31
n-3	5.22±0.15	5.40±0.38
n-6/ n-3	1.34±0.07	1.52±0.19
n-10	13.86±0.97	12.89±0.42
Total *trans*	0.83±0.07	1.02±0.06

[1] identified by standard references and quantified as described in Materials and Methods. Values are obtained in µg/mL considering the GC peak areas recognized and calibrated with standard references (corresponding to >98% of the total peaks of the chromatogram). [2] Values are expressed in percentages relative to the sum of all the quantities of the recognized peaks ± Standard Error of the Mean (s.e.m) from the analyses of n=8 cell samples of each type; statistical significance is estimated: * p value ≤0.045;** p value ≤0.001;*** p value ≤0.0009. Details of the statistical analysis are reported in Materials and Methods.

2.2. Characterization, lipid distribution and fatty acid profiles of EVs released from PC3 and LNCaP cells

EVs were isolated from the cell culture media of the two prostate cancer cell lines, PC3 and LNCaP, using a differential centrifugation method [25,26] and further characterized by electron microscopy and Western blot analyses (Fig. S4 in Supplementary Information). The amount of

released EVs in each preparation was assessed measuring the total protein content and finding similarity for the two cell types ($\sim3\mu g/1 \times 10^6$ cells) (Fig S4A in Supplementary Information). The morphology of purified EVs was examined using Scanning Electron Microscopy (SEM) (Fig. S4B in Supplementary Information). The images revealed the presence of round cup-shaped vesicles with diameters ranging from 50 to 100 nm. Then, the expression of EV marker proteins was evaluated by Western blot (Fig. S4C in Supplementary Information). Isolated EVs and parental cells were probed with positive markers such as tetraspanins (CD9 and CD81) and Alix (protein involved in EV biogenesis) in agreement with guidelines [27]. To exclude contamination with intracellular structures, Western blots for calnexin (marker of endoplasmic reticulum) and actin were also performed. Results showed that EVs from both cell lines contained the two tetraspannins and Alix whereas calnexin and actin were non present (Fig. S4). These results indicated that our EV preparations were devoid of contamination with endoplasmic reticulum or cytoskeletal components and were enriched of vesicles having a size typical of small EVs, consistent with exosomes and/or small membrane microvesicles [26,27]. Moreover, the determination of lipid classes in cells and in their corresponding EVs was performed and the comparison of the lipid distribution showed that EVs have a peculiar composition as compared to their parental cells (Table S1 in Supplementary Information). In both cell lines, the main difference is a higher percentage of cholesterol (CHO, $\approx$13%) and phosphatidylserine (PS, $\approx$26%) in EVs with respect to cells ($\approx$5%), accompanied by a lower percentage of phosphatidyl ethanolamine (PE) and phosphatidyl choline (PC) (Table S1). This finding suggests that EVs may generally express a different lipid composition with respect to their originating cells. These results are in agreement with previous studies on lipid composition of EVs demonstrating that vesicles from different cell types are enriched in CHO, PS and glycosphingolipids with respect to parental cells [21,28,29].

The EVs fatty acid composition of PS, PE, PC was determined as described in Materials and methods, and Table 2 shows the % relative quantities (% rel. quant.) of the fatty acids. The corresponding quantities in $\mu g/mL$ are detailed in Table S2 of Supporting Information. The n-10 family was present in LNCaP derived EVs with percentages similar to the corresponding cell membranes (>12%), and again in both EVs sapienic acid was higher than palmitoleic acid. Interestingly, in PC3 derived EVs the contents of 8cis-C18:1 and sebaleic acid were significantly lower than in EV from LNCaP, thus resulting the total n-10 fatty acid content significantly decreased. It was also found that EVs present a significantly different fatty acid distribution among SFA, MUFA and PUFA families comparing the two cell types, showing that in PC3 derived EVs the MUFA content is increased (+10%), in particular with increase of oleic acid (9*cis*-C18:1), and SFA and PUFA families decreased (−4-5% each) compared to LNCaP. As far as PUFAs are concerned, in PC3-EVs the n-6 family presents significantly less arachidonic acid and the n-3 family presents all its components significantly decreased, thus bringing the n-6/n-3 ratio close to 2. The trans isomer of sapienic acid was significantly higher also in LNCaP-EVs as it was shown for the cell membrane phospholipids. Overall, the differences between the two cell lines were more evident in EVs than in cell membranes.

It is worth recalling that with our analytical methodology, all samples underwent the treatment of dimethyl disulfide (DMDS) derivatization, as previously reported [12,13,17], to unambiguously individuate the position of the double bonds along the chain, thus assessing the presence of the C16 MUFA isomers and the n-10 C18 MUFA and PUFA. In Supplementary Information, Figure S3 shows representative GC chromatograms related to this identification.

Table 2. Fatty acid methyl esters (FAME) (%rel. quant.) obtained from extracellular vesicles (EV) derived from two different prostate cancer cell lines.

FAME[1]	PC3-EVs (n=8)[2]	LNCaP-EVs (n=8)[2]
C14:0	4.38±1.17	5.27±0.25
C16:0	33.32±0.74	35.62±0.96
6*trans*-C16:1	0.10±0.02	0.48±0.03***
6*cis*-C16:1 n-10	6.10±1.59	8.13±0.28
9*cis*-C16:1 n-7	1.10±0.26	1.59±0.08
C18:0	12.35±0.52	15.34±0.66 **
9*trans*-C18:1	0.18±0.04	0.22±0.04
8*cis*-C18:1 n-10	2.85±0.67	4.32±0.27 *
9*cis*-C18:1 n-9	30.83±4.41	15.43±0.66**
11*cis*-C18:1 n-7	1.21±0.08	1.57±0.24
5*cis*,8*cis*-C18:2 n-10	0.25±0.03	0.62±0.07***
mono-trans C18:2 n-6	0.15±0.03	0.20±0.06
C18:2 n-6	3.43±0.50	2.91±0.18
C20:3 n-6	0.49±0.08	0.98±0.16*
C20:4 n-6	0.70±0.15	2.05±0.13***
mono-trans C20:4	0.05±0.02	0.08±0.02
C20:5 n-3	0.29±0.05	0.55±0.09*
C22:5 n-3	0.54±0.14	1.41±0.19**
C22:6 n-3	1.68±0.24	3.22±0.23***
SFA	50.05±1.50	56.23±0.61**
MUFA	42.08±2.25	31.05±0.49***
PUFA	7.39±0.94	11.74±0.41***
n-6	4.62±0.57	5.94±0.22*
n-3	2.51±0.38	5.18±0.32***
n-6/n-3	1.97±0.17	1.18±0.08***
n-10	9.20±2.23	13.07±0.50
Total *trans*	0.48±0.08	0.98±0.09

[1] identified by standard references and quantified as described in Materials and Methods. Values are obtained in µg/mL considering the GC peak areas recognized and calibrated with standard references (corresponding to >98% of the total peaks of the chromatogram). [2] Values are expressed in percentages relative to the sum of all the quantities of the recognized peaks ± Standard Error of the Mean (s.e.m) from the analyses of n=8 cell samples of each type; statistical significance is estimated: *p value ≤0.05; **p value ≤0.003; ***p value ≤0.0006. Details of the statistical analysis are reported in Materials and Methods.

2.3 Characterization of fatty acids-related enzyme expressions in PC3 and LNCaP cells

We also evaluated in PC3 and LNCaP cells the expression of enzymes involved in fatty acids biosynthesis by qRT-PCR, with attention to desaturases and elongases. In Supplementary Information the list of primers used for this analysis is reported in Table S3 (see Supporting Information). The elongation enzymes, involved in the addition of two carbon atoms unit to palmitic acid, are characterized by the acronym ELOVL (Elongation of Very Long chain fatty acids), whereas the desaturation enzymes, involving in the double bond formation, are indicated either by the acronym SCD (Stearoyl CoA desaturase) or FADS (Fatty Acid Desaturase). In Figure 2 the fold-increase or decrease of enzyme expression in PC3 cells is reported with respect to LNCaP cells. We found that FADS3 is expressed at higher level in PC3 cells. Besides, FADS1 (not indicated in

Figure 2) is also expressed at higher level in PC3. It was possible to amplify FADS3 from PC3 cells in standard conditions, whereas only a higher amount of cDNA (x10) and less stringent amplification conditions allowed amplification from LNCaP (data not shown). FADS3 is clustered with family members FADS1 and FADS2 at 11q12-q13.1260 [30]. It is the less characterized member of the desaturase family and even if it is likely to be a desaturase, its exact function remains elusive. It has been implicated in delta-13 desaturation of trans-vaccenic acid (11*trans*-C18:1) [31]. However, FADS3 knockout mouse model confirmed lower desaturase activity, whereas no delta-13 desaturation of vaccenic acid was observed [32]. More recently, evidence has been provided that FADS3 is involved in delta-14 sphingoid base desaturation [33], but this finding needs additional confirmatory studies. FADS1 has a delta-5 desaturase activity, although recent evidence of a delta-7 desaturase activity has also been reported [34]. It is involved in the synthesis of critically important PUFA [35]. FADS3, it is an extensively spliced protein, with at least 8 alternative transcripts that are conserved [35]. Higher levels of FADS1 and FADS3 in PC3 would be expected to be associated with higher level of desaturation. Looking the results of the cell membranes, no significant differences of total MUFA and PUFA levels, unless for the higher level of palmitoleic acid (9*cis*-C16:1) and lower level of n-6 linoleic acid, in PC3 than in LNCaP were detected. Instead, for their released EVs a significantly higher level of total MUFA, in particular oleic acid, was observed in PC3.
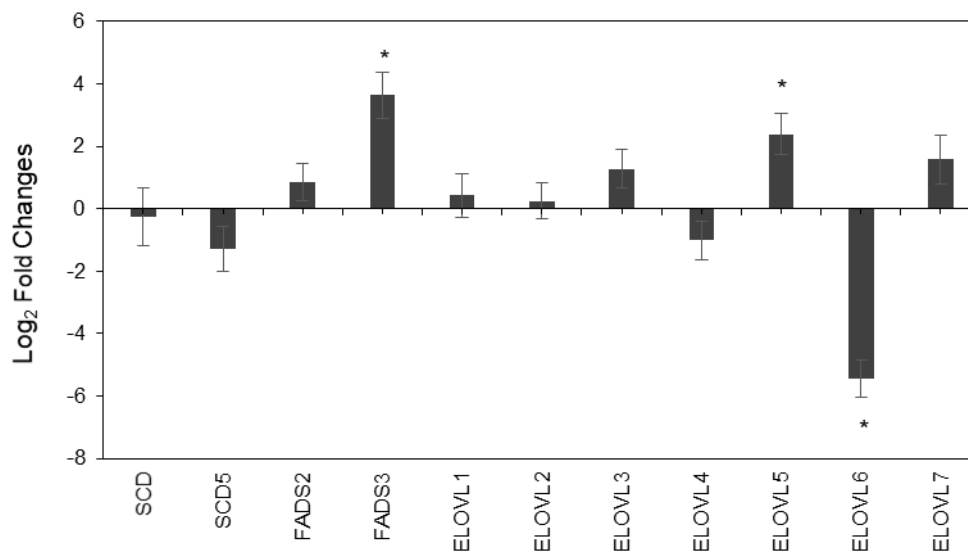

Figure 2. Evaluation of desaturases and elongases expression in PC3 cells by qRT-PCR. X-axis presents 4 desaturase and 7 elongase enzymes. Y axis represents the log2 (fold change) of PC3 with respect to LNCaP cells. Fold change was calculated by $\Delta\Delta CT$ method, using GAPDH as control for ΔCt and calculating $\Delta\Delta Ct$ by subtracting ΔCt for PC3 to ΔCt for LNCaP.

The unclear function of the enzyme isoforms (and genetic polymorphisms) makes it difficult to speculate about the consequences of its higher expression in PC3 cells. Besides, recent findings also suggest that FADS3 might be related to sphingolipid metabolism. As for FADS1, a high number of the functional variants have also been reported to be associated with this gene and their role in affecting long chain PUFA biosynthesis is currently unclear [36]. Besides, FADS1 and FADS2 compete for the same substrates and both cell types show similar level of FADS2.

Analysis of elongases transcripts showed that ELOVL5 was expressed at higher level in PC3 than LNCaP, whereas the level of ELOVL6 was remarkably lower. ELOVL5, together with ELOVL2, is involved in PUFA elongation. ELOVL5 is specific for 18 and 20 carbon fatty acids, whereas ELOVL2 is a C20-24 PUFA elongase [37]. On the other hand, ELOVL6 prefers SFA and MUFA as substrates, elongating fatty acids with 12, 14 and 16 carbons. Similar preferences are shown by ELOVL1, ELOVL3, and ELOVL7, whereas ELOVL4 prefers SFA and very long chain PUFA with 28

to 38 carbons. Consequently, despite its remarkable lower level in PC3 cells, ELOVL6 function in fatty acid elongation may be compensated by ELOVL1, ELOVL3, and ELOVL7, which possess overlapping activity and are comparably expressed between the two cell types [35].

It must be also considered that fatty acids from membrane phospholipids may not reflect only the expression level of enzymes involved in their biosynthesis, but also the activity of enzymes involved in fatty acid remodelling of membrane phospholipids, such as lysophospholipid acyltransferases [38].

3. Discussion

The formation of the n-10 fatty acid series is an emerging pathway in cancer cell metabolism providing MUFA and the de novo PUFA component sebaleic acid (see Figure 1). Sapienic acid, which is the precursor of the n-10 series, was detected for the first time in sebocytes [15] and later it was found in human blood circulating lipids and red blood cell membranes [12,13] as well as in a Caco-2 cell line [17]. It is interesting to note that sapienic acid in Caco-2 cell membrane phospholipids corresponded to 1.6% of the total recognized FA, and the sapienic/palmitoleic ratio was in favor of the latter (1.6/7 = 0.23). By monitoring of Caco-2 cell membrane lipidome after sapienic acid supplementation, it was shown that the n-10 fatty acid metabolism occurs immediately and its metabolites are incorporated as membrane phospholipid fatty acids, i.e., in 30 min as 8cis-C18:1 and in 1 hour as the PUFA sebaleic acid. In the present work we examined fgor the first time PC3 and LNCaP cell lines for the n-10 MUFA and PUFA finding them at a very high percentage (>12%). This is an important result highlighting such metabolism in these cell lines compared to the colon cancer cell line. Indeed, PC3 and LNCaP cell lines present high levels of sapienic acid (> 7%) and a sapienic/palmitoleic acid ratio in favor of the former (ca. 3.5). It is worth noting that in our previous Caco-2 cell line study [17], we found an initial lower n-10 asset, but the sapienic acid supplementation reverted it to reach a sapienic/palmitoleic acid ratio >2.3. It is worth underlining that the palmitic acid partitioning between delta-6 and delta-9 desaturase enzymes is under investigation also for the genetic polymorphisms [39,40]. In a recent paper by Vriens et al [18], sapienic acid was reported in several human cancer cell lines, with increased levels compared to healthy cells. Sapienic acid was discussed as a sign of increased plasticity of cancer cells, however these authors did not follow-up the metabolism of sapienic acid up to sebaleic acid. We can argue that as a sign of plasticity the whole n-10 fatty acid series must be followed up, more importantly if we consider the formation of sebaleic acid as an endogenous PUFA that gives a decisive contribution to fluidity and adaptability features of eukaryotic cells. While the endogenous production of PUFAs cannot occur in eukaryotic cells without dietary supplementation of precursors, sebaleic acid is the only PUFA formed de novo in human cells. Its fate must be addressed in further work, also in order to be associated to a specific cancer cell phenotype, as well as to signaling pathways or plasticity features. It is important to recall that de novo lipogenesis and membrane saturation are interpreted as a "resistance" outcome in cancer cell metabolism [41]. The significant increase of the geometrical trans isomer of sapienic acid in LNCaP cell membranes and EVs can be accounted for an endogenous free radical-based cis-trans isomerization occurring under cellular stress [13,14]. The significance of such data in cancer must be deepened in further work.

Since LNCaP cell line is known to have a less invasive profile than PC3, we can list the observed differences in their membrane lipidomes and EVs, tentatively extrapolating them to tumor proliferative effects, as follows: a) PC3 have a significantly high n-9 MUFA palmitoleic acid in cell membrane and an increase of n-9 oleic acid and total MUFA family in EVs, both considered as invasiveness markers associated with enhanced desaturase enzymatic activities [3,4]; b) in PC3-EVs the total SFA and PUFA contents are significantly lower and total MUFA are significantly higher than LNCaP-EVs, in particular with much lower levels of n-3 for PC3. The latter can indicate loss of molecular factors and related signaling that are known to control prostate cancer invasiveness and aggression [42-44].

It is worth recalling at this point that the mass spectrometry tools for lipidomic research and EVs analysis already evidenced important differences that can be used for diagnostic purposes [21,22]. In our work we could properly address the detection of the n-10 fatty acids that are

positional isomers of MUFA and PUFA present in naturally occurring lipids. Here we propose that this new fatty acid family indicates the increase of MUFA biosynthesis and the EV enrichment could have a role for the transfer of biologically active lipids and lipid metabolites as a mechanism to affect cancer microenvironment. It will be extremely important to understand with further research the correlation between de novo synthesized n-10 fatty acids and the presence of angiogenesis, growth and other metabolism-affecting factors in EVs. Further, the EV cargos enriched by n-10 family could also indicate the transport of MUFA to hypoxic tumoral tissues where the desaturation can be decreased and the subsequent utilization of these fatty acids as substrates for fatty acid oxidation [45]. More work is needed to deepen the roles of these lipids in cancer metabolic plasticity and our findings on the prostate cancer cells indicate an important field of application.

Using PCR analysis for the enzyme expressions in the two different cell lines, we individuated a higher desaturase expression in PC3 cells than in LNCaP, that could combine with the higher level of palmitoleic acid (9*cis*-C16:1), as well as with higher levels of linoleic acid and lower levels of arachidonic acid found in PC3 cell membranes. Since palmitoleic acid is marker of endogenous formation of the double bond in position 9 and linoleic acid is transformed by delta-6 desaturase, these fatty acid levels could have an indirect connection with the found enzymatic expressions. As matter of facts, the significant low levels of arachidonic acid in the most aggressive PC3 cell line could not mean a diminished biosynthesis, but could be a cellular response producing the release of arachidonic acid with its involvement in oxidative and signalling processes, as previously described by some of us for pancreatic cell lines [46]. On the other hand, the released EVs of the two cell lines showed a significantly higher level of MUFA in PC3 than in LNCaP, which opens the possibility that the cellular desaturase increase is then reflected into the corresponding EV composition, also to fulfil the role of cargos as explained above. This can be also true for the reduced elongation activity (ELOVL6) that affects SFA levels in PC3-EVs. The increase of MUFA and decrease of SFA were evaluated in fibroblasts exposed to H-Ras and this was associated to senescence [47], although in that case the identification of the MUFA families was restricted to oleic and palmitoleic acids. On FADS3 recent research highlighted its involvement for the biosynthesis of long chain PUFA, where it was shown that FADS3 desaturase activity reduces elongase expression and activity [32].

Our results on the n-10 fatty acid family encourage further combination with genetic and metabolomic data to expand the comprehension of the fatty acid desaturase activities and influence on the distribution of fatty acids. Indeed, efforts are needed to gather a full understanding of the fatty acid balance reached in specific health conditions, and we believe that the lipid asset including n-10 series is a relevant step forward, in particular to fight cancer invasiveness and survival.

4. Materials and Methods

Sapienic acid methyl ester, 8cis-18:1 methyl ester, sebaleic acid methyl ester were purchased from Lipidox (Lidingö, Sweden); cis and trans FAME, dimethyl disulphide, iodine, cholesterol, sphingomyelin, formic acid acid were purchased from Sigma-Aldrich (San Louis, MO, USA), and used without further purification; chloroform, methanol, isopropanol, diethyl ether and n-hexane, were purchased from Baker (HPLC grade) and used without further purification, POPC, POPE, POPS were purchased from Larodan and used without further purification.

Silica gel analytical thin-layer chromatography (TLC) was performed on Merck silica gel 60 plates, 0.25mm thickness, and spots were detected by spraying the plate with cerium ammonium sulfate/ammonium molybdate reagent.

Fatty acid methyl esters (FAME) were analyzed by GC (Agilent 6850, Milan) in splitless mode, equipped with a 60m × 0.25mm × 0.25μm (50%-cyanopropyl)-methylpolysiloxane column (DB23, Agilent, USA), and a flame ionization detector with the following oven program: temperature started from 165 °C, held for 3 min, followed by an increase of 1 °C/min up to 195 °C, held for 40 min, followed by a second increase of 10 °C/min up to 240 °C, and held for 10min. A constant pressure

mode (29 psi) was chosen with helium as carrier gas. Methyl esters were identified by comparison with the retention times of authentic samples. LOD and LOQ of GC instrument were described in previously works [17]. The FAME are expressed as μg/mL (mean ± S.E.M.) using the calibration procedures previously described [17], and are reported in Table S2 in Supplementary Information as well as in quantitative relative percentages (mean ± S.E.M) (Tables 1-2 in the main text).

Dimethyl disulphide adducts of FAME were analyzed by GC-MS (Thermo Scientific Trace 1300) equipped with a 15m × 0.25mm × 0.25μm TG-SQC 5% phenyl methyl polysiloxane column, with helium as carrier gas, coupled to a mass selective detector (Thermo Scientific ISQ) with the following oven program: temperature started at 80 °C, maintained for 2 min, increased at a rate of 15 °C/min up to 140 °C, increased at a rate of 5 °C/min up to 280 °C and held for 10 min.

Phospholipid classes were analyzed by HPLC (Agilent 1200) equipped with RP18 (Macherey-Nagel EC 150/4.6 Nucleodur C18 HTEC,5 ⊚M) using the following isocratic condition: H_2O +0.2%HCOOH, MEOH 2-Propanolo 10/20/70,detector UV 203. The phospholipids were identified by comparison with the retention times of authentic samples. The values are expressed in μg/mL.

4.1. Cell culture

The human prostatic carcinoma cell lines, PC-3 and LNCaP, were growth in RPMI 1640 medium supplemented with 10% (v/v) heat-inactivated fetal bovine serum (FBS), 2 mM glutamine, 100 μg/mL streptomycin, in a humidified atmosphere containing 5% CO_2 at 37 °C. For experimental purposes, cells (5×10^6cells/10 mL medium) were seeded in 75 cm^2 flasks and, after reaching sub-confluence, the culture medium was carefully removed and the cells were washed twice with phosphate-buffered saline (PBS). Then, cells were maintained for 24h in serum-free medium. At the end of this period, cell culture media were collected to isolate EVs. Cells were recovered and counted by Countess (Countess™ Automated Cell Counter, C10227, Invitrogen). Cell viability was assessed by Trypan Blue stain exclusion.

4.2. EV isolation

EVs were isolated from cell culture media (30 mL) by a differential centrifugation protocol [26,27]. Briefly, media were subjected to low-speed centrifugations to remove cells, cell debris and large EVs ($300g$ for 10 min; $2.000g$ for 20 min; $10.000g$ for 30 min). The supernatants were ultracentrifuged at 100.000 g for 70 min to pellet EVs, which was washed in PBS and centrifuged again at $100.000g$ for 70 min. EV pellets were re-suspended in small volume of PBS (150 μL) and used for further analyses.

4.3. Scanning electron microscopy

For scanning electron microscopy (SEM) examination, EVs were fixed in 2.5% glutaraldehyde for 15 min at room temperature, washed twice with large volume of water using Vivaspin concentration devices (300,000 Da cut-off), then sedimented on glass coverslips and allowed to dry at room temperature. SEM images were obtained using a field emission gun electron scanning microscope (LEO 1525 Zeiss; Thornwood, NY, USA) after Cr metallization using a high- resolution sputter Q150T ES-Quorum apparatus (24 sec. sputter at a current of 240 mA). Chromium thickness was ~10 nm.

4.4. Western blotting

For Western blotting analyses, cells were recovered, washed twice with PBS and centrifuged again. Approximately 3×10^6 cells were lysed at 4°C in RIPA buffer (50 mM Tris-HCl pH 8, 150 mM NaCl, 1% (v/v) NP-40, 0.1% (w/v) SDS, 0.5% (w/v) sodium deoxycholate) in the presence of a protease inhibitor mixture. Insoluble material was removed by centrifugation at $13,000g$ for 10 min at 4°C.

Aliquots of cell lysates (10-30 μg) or EVs (5 μg) were mixed with sample buffer 5X (1M Tris-HCl pH 6.8, 5% (w/v) SDS, 6% (v/v) glycerol, 0.01% (w/v) Bromophenol blue) without DTT (non-reducing conditions, used for CD9 detection according to manufacturer's instructions) or with 125 mM DTT (used for the other antibodies). Samples were boiled for 5 min, electrophoresed on 12% acrylamide gel and electrotransferred to PVDF membrane. After 30 min incubation at RT with blocking buffer (5% BSA in TBS-Tween) membranes were incubated overnight with the following primary antibodies: goat polyclonal anti-Alix (Santa Cruz, USA), mouse monoclonal anti-CD9 (Abcam, Cambridge, UK), mouse monoclonal anti-CD81 (Santa Cruz, USA), goat polyclonal anti-calnexin (Sigma-Aldrich, St Louis, USA), anti β-actin (Sigma-Aldrich, St Louis, USA).

4.5. Quantitative PCR

RNA was extracted using Trifast reagent (Euroclone), according to the manufacturer's instructions. 1 μg of RNA was reverse-transcribed into cDNA using random hexamers and SuperScript II Reverse Transcriptase (Life Technologies, Carlsbad, CA, USA). cDNA was used to determine transcript levels by qRT-PCR in a StepOne RT-PCR machine (Applied Biosystems, USA) using SYBR® Select Master Mix (Life Technologies). Primers used are listed in Supplementary Table S3. GADPH used as endogenous control was amplified with primers 5'-GAG AAG GCT GGG GCT CAT TT (forward) and 5'-AGT GAT GGC ATG GAC TGT GG (reverse). Data were analysed using the $\Delta\Delta C_t$ method. ΔC_t was calculated subtracting the average C_t value of GADPH as control to the average C_t value of each transcript for PC3 and LnCaP. $\Delta\Delta C_t$ is the difference between the ΔC_t for each transcript for PC3 and the ΔC_t of each transcript for LnCaP as control. The reported fold expression, expressed as RQ (Relative Quantity), was calculated by $2^{-\Delta\Delta C_t}$. The analysis was repeated three times in triplicate. The mean ± S.D. of a representative experiment is reported (*$p<0.05$).

4.7. Membrane lipid characterization, extraction and fatty acid analysis of PC3 cells, LNCaP cells and their corresponding extracellular vesicles.

To the pellets of PC3 cells (3×10^6 cells) and LNCaP cells (3×10^6 cells) tridistilled water (1 mL) was added and samples were centrifuged at 14000 rpm for 15 minutes at 4C°; the supernatant was discarded and the pellets were re-suspended in 1 mL of tridistilled water. An aliquot of 20 ◎l was used for the HPLC analysis of phospholipid classes (Table S1 in Supplementary Information), and the rest of the suspension was extracted with 2:1 chloroform/methanol (4× 4mL) according to the Folch method [48]. The organic layers were dried on anhydrous Na_2SO_4 and evaporated to dryness. The total lipid extracts (0.6-0.7 mg) were analysed by TLC (*n*-hexane:diethyl ether 9:1) for their composition confirming the presence of phospholipids and cholesterol as the main components. The extracts were converted to FAME (fatty acid methyl esters) by adding 0.5 M KOH in MeOH (0.5 mL). After 10 minutes the reaction was quenched by brine (0.5 mL) and FAME were extracted with n-hexane (4×2 mL), dried on anhydrous Na_2SO_4, evaporated to dryness. GC analysis was performed using standard references for peak identification and quantitation. Extracellular vesicles were worked up as described for cell samples, except for the centrifugation step, since the samples (300 μL/100 μg proteins) were added with tridistilled water (0.3 mL) and centrifuged at 30000 rpm for 1.5 h at 4C° in order to separate the pellet.

4.8. DMDS derivatization

The FAME mixture obtained from PC3, LNCap cells and EVs followed a previously described procedure for the derivatization and GC/MS analysis in order to proceed with the assignment of the double bond position [17]. Briefly, in a Wheaton vial containing FAME dissolved n-hexane (50μL), 70μL of dimethyl disulfide and 2 drops of a 6% solution of iodine in diethyl ether were consecutively added. The reaction was stirred at room temperature for 1.5 h under argon atmosphere. Then, 1 mL of n-hexane and 1 mL of a 5% aqueous solution of sodium thiosulphate were consecutively added. The organic phase was isolated, dried over anhydrous Na_2SO_4, and concentrated under gentle

stream of nitrogen, before the GC-MS analysis (Figure S3 in Supporting Information shows a representative example of GC analyses).

4.9.Statistical analysis.

For statistical analysis the fatty acids were expressed in relative percentages and expressed as mean ± S.E.M. (standard error of the mean). Statistical analysis was performed using GraphPad Prism 5.0 software (GraphPad Software, Inc., San Diego, CA). We used non-parametric unpaired t-test two-tailed with 95% confidence interval.

5. Conclusions

The detailed fatty acid characterization for each cancer cell type can afford interesting information, envisaging important applications not only for molecular biology studies but also for clinical and nutritional research applications. Fatty acids are a relevant part of the metabolism and the diet and can offer escaping strategies for cell survival. Since delta-6 desaturase partitioning between palmitic acid for sapienic acid formation and dietary PUFAs is not yet disclosed, the characterization of the fatty acid profiles and the contribution of n-10 series in specific cancer cell lines is relevant to fully understand metabolic pathways and individuate anticancer strategies. Indeed, this information could be useful to design lipid therapies with n-6/n-3 PUFA supplementation, tailored to balance the n-10 fatty acid formation. Fatty acid-based functional lipidomics with isomers detection can bring important information that is extendable to personalized molecular profiles and nutritional approach for cancer patients. It is known that PUFA are regulators of several metabolic pathways and signaling related to cancer [49-52], therefore it is timing to afford a complete scenario that helps in the overall comprehension of the balance between n-7, n-9 and n-10 fatty acid series with n-6 and n-3 dietary contribution. Our results are relevant to improve the present knowledge in cancer phenotype and diagnostics, highlighting EV lipidomics to monitor positional fatty acid isomer profiles and MUFA levels in cancer.

Supplementary Materials: The following are available online at www.mdpi.com/xxx/s1. Figure S1. Representative GC chromatogram of fatty acid methyl esters obtained from PC3 membrane phospholipids. In the boxes the enlargement of the areas containing C16 MUFA (green box) and 8*cis*-C18:1, 5*cis*,8*cis*-C18:2 (purple box). Figure S2. Representative examples of FAME analyses coming from phospholipids of A, (LnCap cells), B (EVs Lncap) and C (EVs PC3). Figure S3. Representative GC/MS analyses of FAME mixture obtained from membrane phospholipids of the A, (PC3) and B (LNCaP) after DMSD derivatization following the protocol described in Materials and Methods; GC/MS traces focus on the chromatographic region containing the FAME DMDS adducts of: 6*cis*-C16:1, 9*cis*-C16:1 , *cis*8-C18:1, *cis*9-C18:1 and *cis*5,*cis*8-C18:2; in the bottom, the box contains details of the diagnostic fragmentations of the DMDS adducts, and the color codes indicate these fragments and their detection in the samples. Figure S4. Characterization of EVs released by PC3 and LNCaP cells. EVs were isolated from cell culture media of PC3 or LNCaP cells by differential centrifugation (see Materials and Methods). A) Recovered EVs quantified as µg proteins/10^6 cells (mean+S.D., n=8). B) Scanning electron micrographs of EVs. See Materials and Methods for experimental details. C) Cell lysates and EV preparations were separated by SDS-PAGE, electrotransferred and probed with the indicated positive and negative EV markers. See Materials and Methods for experimental details. Table S1: Main lipid classes detected in PC3 and LNCaP cell membranes and their corresponding EVs expressed in µg/mL and reported as mean ± SEM. In the brackets are reported results expressed as percentage of the sum of all identified lipids (*EVs *vs* corresponding cells). Table S2. Membrane phospholipid fatty acids of PC3 cells, PC3-EVs, LNCaP cells and LNCaP-EVs expressed in µg/mL. These data were used for the values in Tables 1 and 2 expressed as % relative quantitative (% rel. quant.). Table S3. Primers used for qRT-PCR.

Author Contributions: Conceptualization, C.F; methodology, C.F. and S.B.; formal analysis, A.S., E.C., L.U.; data curation, C. F., S. B., A. S.; writing—original draft preparation, C.F.; writing—review and editing, C.F., A.S., S. B.,C.C., C.E.; supervision, C.F., C.C.; funding acquisition, C.F., S.B.,C.E., C.C.
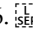
Abbreviations

CHO Cholesterol
DMDS Dimethyl disulphide
ELOVL Elongation enzyme
EV Extracellular vesicle
FADS Fatty acid desaturase
FAME Fatty acid methyl esters
FBS Fetal bovine serum
GC Gas chromatography
HPLC High performance liquid chromatography
MUFA Monounsaturated fatty acids
PBS Phosphate buffered saline
PC Phosphatidyl choline
PE Phosphatidyl ethanolamine
PS Phosphatidyl serine
PL Phospholipid
PUFA Polyunsaturated fatty acids
SFA Saturated fatty acids
SF Sphingomyelin
SCD Stearoyl CoA desaturase
TLC Thin layer chromatography

References

1. Baenke, F.; Peck, B.; Meiss, H.; Schulze, A. Hooked on fat: the role of lipid synthesis in cancer metabolism and tumour development. *Dis. Model. Mech.* **2013**, *6*, 1353–1363; DOI:10.1242/dmm.011338.
2. Röhrig, F.; Schulze, A. The multifaceted roles of fatty acid synthesis in cancer. *Nature Rev. Cancer* **2016**, *16*, 732–749.
3. Igal, R.A. Roles of Stearoyl Coa Desaturase-1 in the Regulation of Cancer Growth, Survival and tumorigenesis. *Cancer* **2011**, *3*, 2462–2477; DOI:10.3390/cancers3022462.
4. Kamphorst, J. J.; Cross, J. R.; Fan, J.; Methew, R.; White, E. P.; Thompson, C.B.; Rabinowitz, J. D. Hypoxic and Ras-transformed cells support growth by scavenging unsaturated fatty acids from lysophospholipids. *Proc. Natl. Acad. Sci. USA* **2013**, *110*, 8882–8887; DOI: 10.1073/pnas.1307237110.
5. Peck, B.; Schug, Z. T.; Zhang, Q.; Dankworth, B.; Jones, D.T.; Smethurst, E.; Patel, R.; Mason, S.; Jiang, M.; Saunders, R.; Howell, M.; Mitter, R.; Spencer-Dene, B.; Stamp, G.; McGarry, L.; James, D.; Shanks, E.; Aboagye, E. O.; Critchlow, S. E.; Leung, H. Y.; Harris, A. L.; Wakelam, M. J. O.; Gottlieb, E.; Schulze, A. Inhibition of fatty acid desaturation is detrimental to cancer cell survival in metabolically compromised environments. *Cancer Metab.* **2016**, *4*, 6; DOI: 10.1186/s40170-016-0146-8.
6. Mason, P.; Liang, B.; Li, L.; Fremgen, T.; Murphy, E.; Quinn, A.; Madden, S. L.; Biemann, H. P.; Wang, B.; Cohen, A.; Komarnitsky, S.; Jancsics, K.; Hirth, B.; Cooper, C. G.; Lee, E.; Wilson, S.; Krumbholz, R.; Schmid, S.; Xiang, Y.; Booker, M.; Lillie, J.; Carter, K. SCD1 inhibition causes cancer cell death by depleting mono-unsaturated fatty acids. *PLoS One* **2012**, 7, e33823; DOI: 10.1371/journal.pone.0033823.
7. Cao, H.; Gerhold, K.; Mayers, J. R.; Wiest, M. M.; Watkins, S. M.; Hotamisligil, G. S. Identification of a lipokine, a lipid hormone linking adipose tissue to systemic metabolism. *Cell* **2008**, *134*, 933−944; DOI: 10.1016/j.cell.2008.07.048.
8. Koeberle, A.; Shindou, H.; Harayama, T.; Shimizu, T. Palmitoleate is a mitogen, formed upon stimulation with growth factors, and converted to palmitoleoyl phosphatidylinositol. *J. Biol. Chem.* **2012**, *287*, 27244−27254.

9.   Astudillo, A. M.; Meana, C.; Guijas, C.; Pereira, L.; Lebrebro, P.; Balboa, M. A.; Balsinde, J. Occurrence and biological activity of palmitoleic isomers in phagocytic cells. *J. Lipid Res.* **2018**, *59*, 237–249.

10.   Warensjo, E.; Rosell, M.; Hellenius, M. L.; Vessby, B.; De Faire, U.; Riserus, U. Associations between estimated fatty acid desaturase activities in serum lipids and adipose tissue in humans: links to obesity and insulin resistance. *Lipids Health Dis.* **2009**, *8*, 37; doi: 10.1186/1476-511X-8-37.

11.   Lu, Y.; Vaarhorst, A.; Merry, A.H.; Dolle, M.E.; Hovenier, R.; Imholz, S.; Schouten, J.L.; Heijmans, B.T.; Müller, M.; Slagboom, P. E.; et al. Markers of endogenous desaturase activity and risk of coronary heart disease in the CAREMA cohort study. *PLoS One* **2012**, *7*, e41681; doi: 10.1371/journal.pone.0041681.

12.   Sansone, A.; Melchiorre, M.; Chatgilialoglu, C; Ferreri, C. Hexadecenoic fatty acid isomers: a chemical biology approach for human plasma biomarker development. *Chem. Res. Toxicol.* **2013**, *26*, 1703–1709.

13.   Sansone, A.; Tolika, E.; Louka, M.; Sunda, V.; Deplano, S.; Melchiorre, M.; Anagnostopoulos, D.; Chatgilialoglu, C.; Formisano, C.; Di Micco, R.; et al. Hexadecenoic Fatty Acid Isomers in Human Blood Lipids and Their Relevance for the Interpretation of Lipidomic Profiles. *PLoS One* **2016**, *11*, e0152378; doi: 10.1371/journal.pone.0152378.

14.   Chatgilialoglu, C.; Ferreri, C.; Melchiorre, M.; Sansone, A.; Torreggiani, A. Lipid geometrical isomerism: from chemistry to biology and diagnostics. *Chem. Rev.* **2014**, *114*, 255–284.

15.   Prouty, S. M.; Pappas, A. Sapienic acid: species-specific fatty acid metabolism of human sebaceous gland. In *Lipids and Skin Health*; Pappas, A. Ed.; Springer International Publisher: New York, USA, 2015, pp. 139-157; doi:10.1007/978-3-319-09943-9_10.

16.   McNairn, A.J.; Doucet, Y.; Demaude, J.; Brusadelli, M.; Gordon, C. B.; Uribe-Rivera, A.; Lambert, P. F.; Bouez, C.; Breton, L.; Guasch, G. TGFβ signaling regulates lipogenesis in human sebaceous glands cells. *BMC Dermatol.* **2013,** *13*, 2; doi:10.1186/1471-5945-13-2.

17.   Scanferlato, R.; Bortolotti, M.; Sansone, A.; Chatgilialoglu, C.; Polito, L.; De Spirito, M.; Maulucci, G.; Bolognesi, A.; Ferreri, C. *Int. J. Mol. Sci.* **2019**, *20*, 832; doi: 10.3390/ijms20040832.

18.   Vriens, K.; Christen, S.; Parik, S.; Broekaert, D.; Yoshinaga, K.; Talebi, A.; Dehairs, J,; Escalona-Noguero, C.; Schmieder, R.; Cornfield, T.; Charlton, C.; Romero-Pérez, L.; Rossi, M.; Rinaldi, G.; Orth, M. F.; Boon, R.; Kerstens, A.; Kwan, S. Y.; Faubert, B.; Méndez-Lucas, A.; Kopitz, C. C.; Chen, T.; Fernandez-Garcia, J.; Duarte, J. A. G.; Schmitz, A. A.; Steigemann, P.; Najimi, M.; Hägebarth, A.; Van Ginderachter, J. A.; Sokal, E.; Gotoh, N.; Wong, K. K.; Verfaillie, C.; Derua, R.; Munck, S.; Yuneva, M.; Beretta, L.; DeBerardinism R. J.; Swinnen, J. V.; Hodson, L.; Cassiman, D.; Verslype, C.; Christian, S.; Grünewald, S.; Grünewald, T. G. P.; Fendt, S. M. Evidence for an alternative fatty acid desaturation pathway increasing cancer plasticity. Nature **2019**, 566, 403–406.

19.   Peck, B.; Schug, Z. T.; Zhang, Q.; Dankworth, B.; Jones, D. T.; Smethurst, E.; Patel, R.; Mason, S.; Jiang, M.; Saunders, R.; Howell, M.; Mitter, R.; Spencer-Dene, B.; Stamp, G.; McGarry, L.; James, D.; Shanks, E.; Aboagye, E. O.; Critchlow, S. E.; Leung, H. Y.; Harris, A. L.; Wakelam, M. J. O.; Gottlieb, E.; Schulze, A. Inhibition of fatty acid desaturation is detrimental to cancer cell survival in metabolically compromised environments. *Cancer Metab.* **2016**, *4*, 6; doi: 10.1186/s40170-016-0146-8.

20.   Rajagopal, C.; Harikumar, K. B. The origin and functions of exosomes in cancer. *Front. Oncol.* **2018**, *8*, 66; doi: 10.3389/fonc.2018.00066.

21.   Llorente, A.; Skotland, T.; Sylvanne, T.; Kauhanen, D.; Rog, T.; Orlowski, A.; Vattulainen, I.; Ekroos, K.; Sandvig, K. Molecular lipidomics of exosomes released by PC-3 prostate cancer cells. *Biochim. Biophys. Acta* **2013**,*1831*, 1302–1309.

22.   Brzozowski, J.S.; Helen Jankowski, H.; Bond D. R.; McCague, S.; Munro, B.R.; J. Predebon, M.J.; Scarlett, C.J.; Skelding, K.A.; Weidenhofer, J. Lipidomic profiling of extracellular vesicles derived from prostate and prostate cancer cell lines. *Lipids Health Dis*. **2018**, *217*, 1–12. doi: 10.1186/s12944-018-0854-x.

23.   Seim, I.; Jeffery, P. L.; Thomas, P. B.; Nelson, C. C.; Chopin, L. K. Whole-Genome Sequence of the Metastatic PC3 and LNCaP Human Prostate Cancer Cell Lines. *G3 (Bethesda)* **2017**, *7*, 1731–1741.

24.   Tai, S; Sun Y.; Squires, J. M.; Zhang, H.; Oh, W.K.; Liang, C.Z.; Huang, J. PC3 is a cell line characteristic of prostatic small cell carcinoma. *Prostate* **2011**, 71: 1668–1679.

25.   Théry, C; Amigorena, S.; Raposo, G.; Clayton A. Isolation and characterization of exosomes from cell culture supernatants and biological fluids. *Curr. Protoc. Cell Biol.* **2006**, Chapter 3, Unit 3.22. doi: 10.1002/0471143030.cb0322s30.

26.   Kowal, J.; Arras, G.; Colombo, M; Jouve, M.; Morath, J.P.; Primdal-Bengtson, B.; Dingli, F.; Loew, D.; Tkach, M.; Théry, C. Proteomic comparison defines novel markers to characterize heterogeneous populations of extracellular vesicle subtypes. *Proc. Natl. Acad. Sci. USA*. **2016**, 113, E968-77. doi: 10.1073/pnas.1521230113;

27. Lotvall, J.; Hill, A.F.; Hochberg, F.; Buza´s, E.I.; Di Vizio, D.; Gardiner C.; et al. Minimal experimental requirements for definition of extracellular vesicles and their functions: a position statement from the International Society for Extracellular Vesicles. *J. Extracell. Ves.* **2014**, *3*, 26913; https://doi.org/10.3402/jev.v3.26913.

28. Buratta, S.; Urbanelli, L.; Sagini, K.; Giovagnoli, S.; Caponi, S.; Fioretto, D.; Mitro, N.; Caruso,D.; Emiliani, C. Extracellular vesicles released by fibroblasts undergoingH-Ras induced senescences how changes in lipid profile. *Plos One* **2017**, *28*,1-23; doi.org/10.1371/journal.pone.0188840.

29. Lydic, O.A.; Townsend, S.; Adda, C.G.; Collins, C.; Mathivanan, S.; Reid, G.E. Rapid and Comprehensive 'Shotgun' Lipidome Profiling of Colorectal Cancer Cell Derived Exosomes. *Methods* **2015**, *87*, 83-95; doi: 10.1016/j.ymeth.2015.04.014

30. Marquardt, A.; Stöhr, H.; White, K.; Weber, B.H.F. cDNA cloning, genomic structure, and chromosomal localization of three members of the human fatty acid desaturase family. *Genomics* **2000**, *66*, 176-183.

31. Garcia, C.; Duby, C.; Catheline, D.; Toral, P.G.; Bernard, L.; Legrand, P.; Rioux, V. Synthesis of the suspected trans-11,cis-13 conjugated linoleic acid isomer in ruminant mammary tissue by FADS3-catalyzed Δ13-desaturation of vaccenic acid. *J. Dairy Sci.* **2017**, *100*, 783-796.

32. Zhang, J.Y.; Qin, X-; Liang, A.; Kim, E.; Lawrence, P.; Park, W.J.; Kothapalli, K.S.D.; Brenna, J.T. Fads3 modulates docosahexaenoic acid in liver and brain. *Prostaglandins Leukot, Essent, Fatty Acids* **2017**, *123*, 25-32.

33. Karsai, G.; Lone, M.; Kutalik, Z.; Brenna, J.T.; Li, H.; Pan, D.; von Eckardstein, A.; Hornemann, T. FADS3 is a delta14Z sphingoid base desaturase that contributes to gender differences to the human plasma sphingolipidome. *J. Chem. Biol.* **2019,** in press as manuscript AC119.011883

34. Park, H.G.; Engel, M.G.; Vogt-Lowell, K.; Lawrence, P.; Kothapalli, K.S.; Brenna, J.T. The role of fatty acid desaturase (FADS) genes in oleic acid metabolism: FADS1 Δ7 desaturates 11-20:1 to 7,11-20:2. *Prostaglandins Leukot. Essent. Fatty Acids* **2018**, *128*, 21-25.

35. Zhang, J.Y.; Kothapalli, K.S.; Brenna, J.T. Desaturase and elongase-limiting endogenous long-chain polyunsaturated fatty acid biosynthesis. *Curr. Opin. Clin. Nutr. Metab. Care* **2016**, *19*, 103-110.

36. Lattka, E.; Illig, T.; Koletzko, B.; Heinrich, J. Genetic variants of the FADS1 FADS2 gene cluster as related to essential fatty acid metabolism. *Curr. Opin. Lipidol.* **2010**, *21*, 64-69.

37. Guillou, H.; Zadravec, D.; Martin, P.G.; Jacobsson, A. The key roles of elongases and desaturases in mammalian fatty acid metabolism: Insights from transgenic mice. *Prog. Lipid Res*. **2010**, *49*, 186-199.

38. Yamashita, A.; Hayashi, Y.; Nemoto-Sasaki, Y.; Ito, M.; Oka, S.; Tanikawa, T.; Waku, K.; Sugiura, T. Acyltransferases and transacylases that determine the fatty acid composition of glycerolipids and the metabolism of bioactive lipid mediators in mammalian cells and model organisms. *Prog. Lipid Res.* **2014**, *53*, 18-81.

39. Park, H. G.; Kothapalli, K. S. D.; Park, W. J.; DeAllie, C.; Liu, L.; Liang, A.; Lawrence, P.; Brenna, J. T. Palmitic acid (16:0) competes with omega-6 linoleic and omega-3 α-linolenic acids for FADS2 mediated Δ6-desaturation. *Biochim. Biophys. Acta* **2016**, *1861*, 91–97.

40. Byberg, L.; Kilander, L.; Warensjö Lemming E.; Michaëlsson, K.; Vessby, B. Cancer death is related to high palmitoleic acid in serum and to polymorphisms in the SCD-1 gene in healthy Swedish men. *Am. J. Clin. Nutr.* **2014**, *99*, 551–558.

41. Rysman, E.; Brusselmans, K.; Scheys, K.; Timmermans, L.; Derua, R.; Munck, S.; Van Veldhoven, P.P.;Waltregny, D.;Daniëls, V.W.; Machiels,J.; Vanderhoydonc, F.; Smans, K.; Waelkens, E., Verhoeven, G.; Swinnen, J.V. De novo lipogenesis protects cancer cells from free radicals and chemotherapeutics by promoting membrane lipid saturation. *Cancer Res.* **2010**, *70*, 8117–8126.

42. Fabian, C. J.; Kimler, B. F.; Hursting, S. D. Omega-3 fatty acids for breast cancer prevention and survirorship. *Breast Cancer Res.* **2015**, *17*, 62; DOI: 10.1186/s13058-015-0571-6.

43. Friedrichs, W.; Ruparel, S. B.; Marciniak, R. A.; deGraffenried, L. Omega-3 fatty acid inhibition of prostate cancer progression to hormone independence is associated with suppression of mTOR signaling and androgen receptor expression. *Nutr. Cancer* **2011**, *63*, 771–777.

44. Berquin, I.M.; Edwards, I. J.; Kridel, S. J. Chen YQ. Polyunsaturated fatty acid metabolism in prostate cancer. *Cancer Metast. Rev.* **2011**, *30*, 295–309.

45. Lazar, I.; Clement, E.; Attane, C.; Muller, C.; Nieto, L. A new role for extracellular vesicles: how small vesicles can feed tumors' big appetite. *J. Lipid Res.* **2018**, *59*, 1793–1804.

46.   Cohen, G.; Riahi, Y.; Shamni, O.; Guichardant, M.; Chatgilialoglu, C.; Ferreri, C.; Kaiser, N.; S. Sasson. The role of lipid peroxidation and PPARδ in amplifying glucose-stimulated insulin secretion. *Diabetes*, **2011**, *60*, 2830–2842.

47.   Sagini, K.; Urbanelli, L.; Costanzi, E.; Mitro, N.; Caruso, D.; Emiliani, C.; Buratta, S. Ocongenic H-Ras expression indices fatty acid profile changes in human fibroblasts and extracellular vesicles. *Int. J. Mol. Sci.* **2018**, *19*, 3515; doi:10.3390/ijms19113515.

48.   Folch, J.; Less, M.; Sloane Stanley, G. H. A simple method for the isolation and purification of total lipids from animal tissues. *J. Biol. Chem.* **1957**, *226*, 497–509.

49.   Liang, P.; Henning, S. M.; Guan, J.; Grogan, T.; Elashoff, D.; Cohen, P.; Aronson, W. J. Effect of dietary omega-3 fatty acids on castrate-resistant prostate cancer and tumor-associated macrophages. *Prostate Cancer Prostatic Dis.* **2019**, doi:10.1038/s41391-019-0168-8.

50.   Chajès, V.; Bougnoux, P. Omega-6/omega-3 polyunsaturated fatty acid ratio and cancer. In *Omega-6/Omega-3 Essential Fatty Acid Ratio: The Scientific Evidence*; Simoupoulos, A. P.; Cleland, L. G., Eds.; Karger: Basel, Switzerland, 2003; Volume 92, pp. 133–215.

51.   Ferreri, C.; Chatgilialoglu, C. *Membrane Lipidomics for Personalized Health*. John Wiley & Sons: New York, 2015.

52.   Freitas, R.; Campos, M. M. Protective Effects of Omega-3 Fatty Acids in Cancer-Related Complications. *Nutrients* **2019**, *11*, 945; doi:10.3390/nu11050945.